Supplementary data

Assembly and analysis of eukaryotic Argonaute-RNA complexes in microRNA-target recognition

Hin Hark Gan[1,*] and Kristin C. Gunsalus[1,2,*]

[1]Center for Genomics and Systems Biology, Department of Biology, New York University, 12 Waverly Place, New York, NY 10003

[2]New York University Abu Dhabi, Abu Dhabi, UAE

[*]Corresponding author

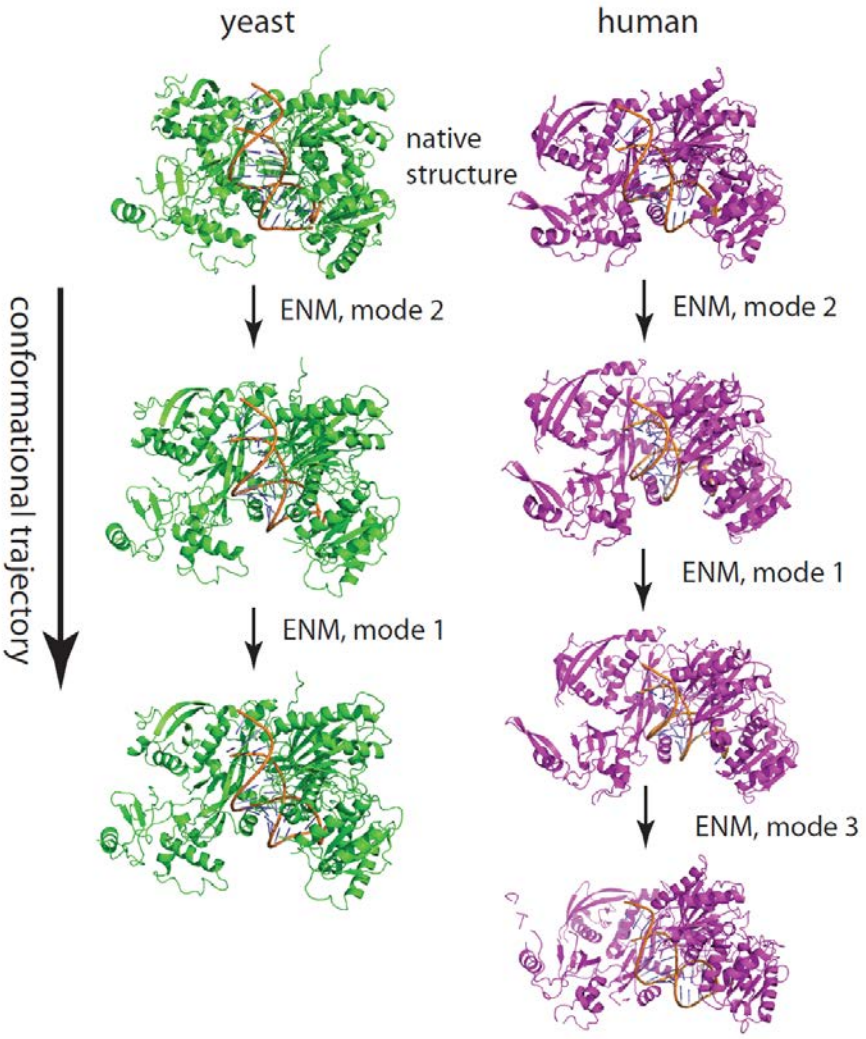

Supplementary Figure S1. A stepwise approach to Ago loading using global conformational moves. Initially, a native Ago structure in the closed conformation is used. The ENM method is then used to generate global Ago conformational moves. A conformation from dynamic modes 1, 2 or 3 is chosen and tested for its ability to fit an RNA-DNA hybrid duplex (3HJF). Improvement of duplex fitting can be made by further conformational moves based on the current conformation by repeating the previous steps. This approach to Ago loading defines a discrete conformational trajectory to achieve correct fitting of a given duplex. As illustrated, yeast Ago loading can be achieved in two conformational moves, whereas the human Ago requires three.

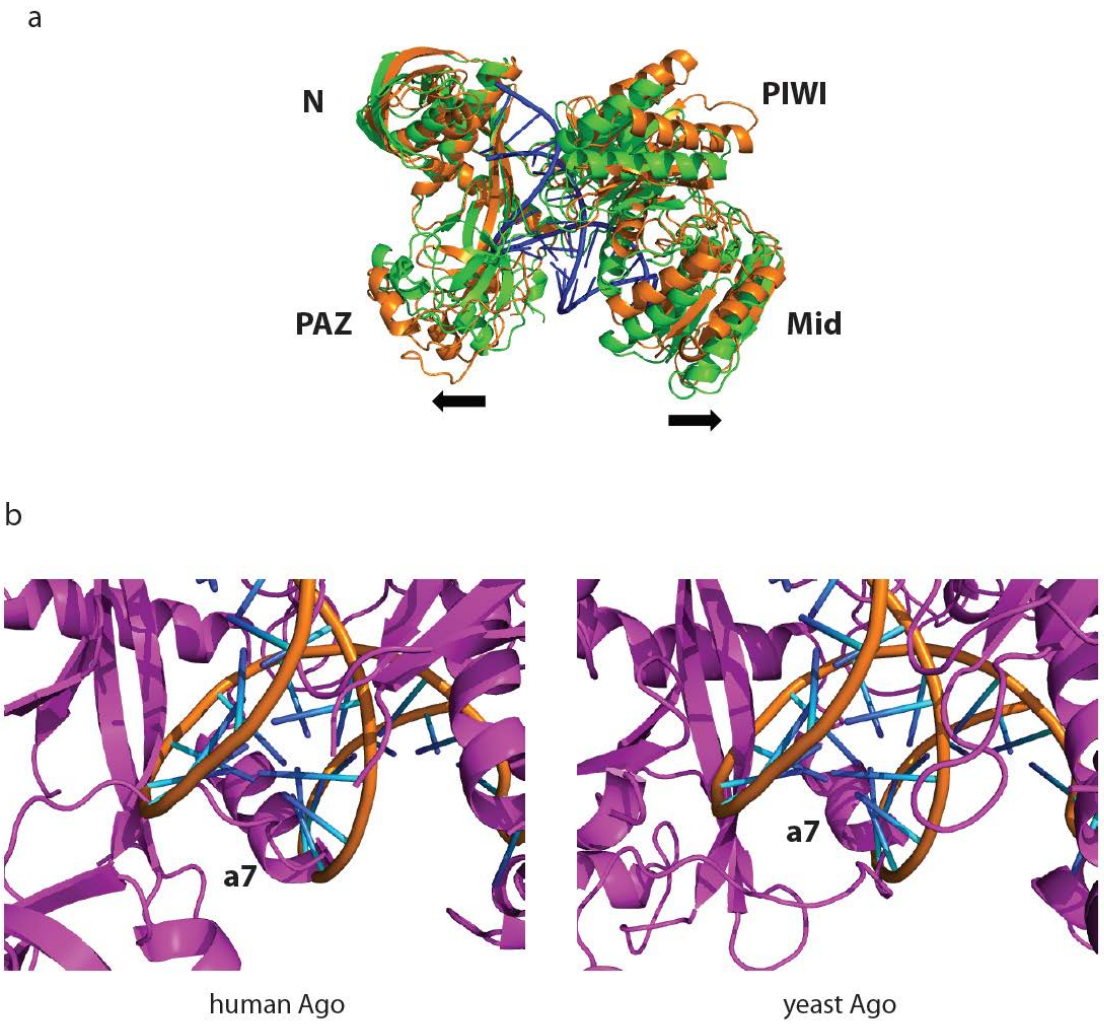

Supplementary Figure S2. Crystal structures of bacterial, yeast and human Argonautes.

a) Superimposed *T. thermophilus* Ago structures with a guide DNA strand (PDB code 3DLH; Ago in green) and hybrid DNA-RNA duplex (3HJF; Ago in orange, duplex in blue); the RMSD value is 2.9 Å. 3DLH is in a closed conformational state, whereas 3HJF is in an open state.

b) Steric clashes arising from loading a hybrid DNA-RNA duplex into solved yeast (4F1N) and human (4EI1) Ago structures; a7 helix in Ago's L2 region is likely destined to fit in the minor groove. The duplex was placed by aligning the eukaryotic Ago structures with the reference *T. thermophilus* Ago structure.

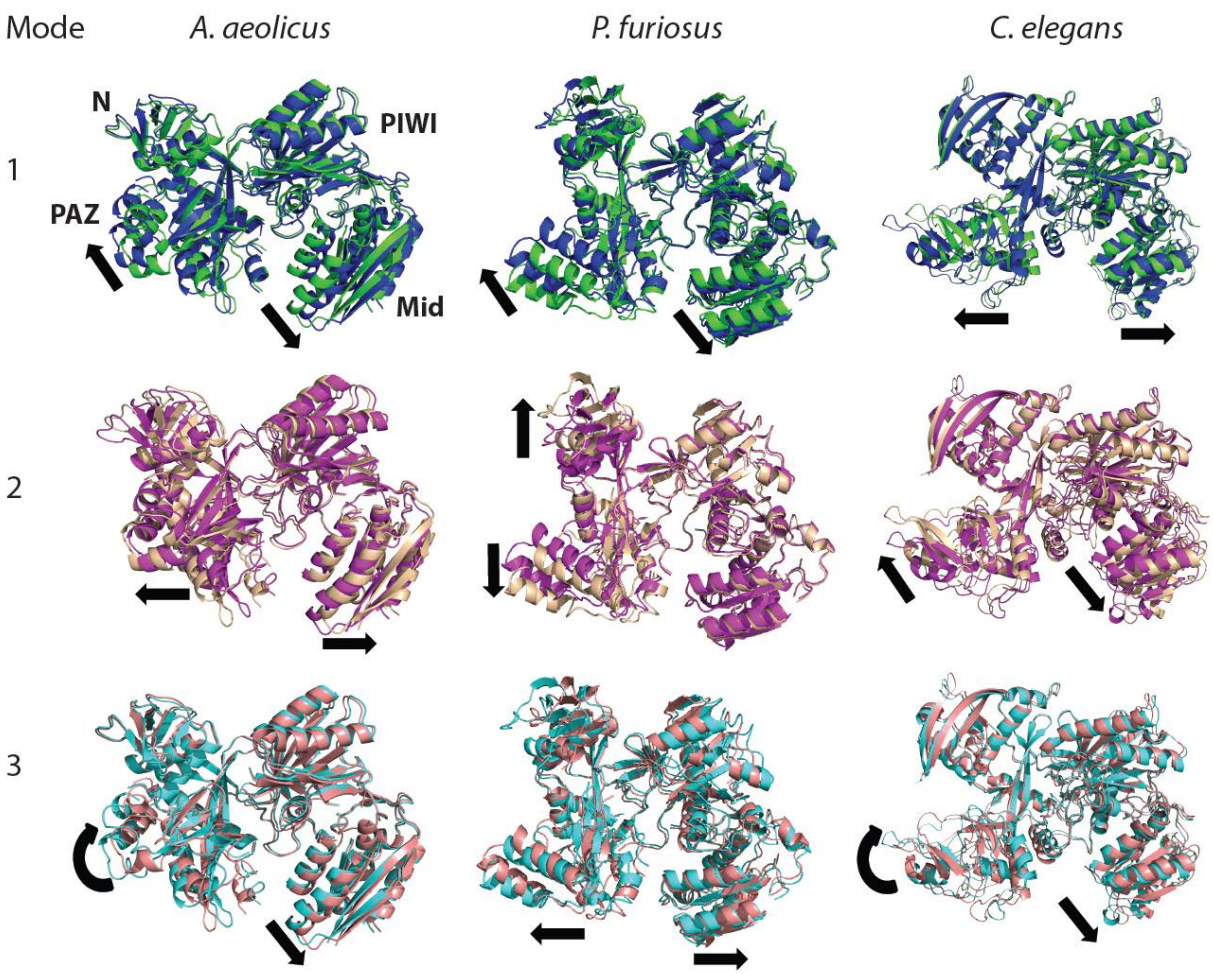

Supplementary Figure S3. Low-frequency conformational dynamics of *A. aeolicus* (PDB code: 1YVU; kingdom: bacteria), *P. furious* (1U04; archaea), and *C. elegans* (modeled ALG-2; eukaryota) Ago structures. These modes of motion are also observed in *T. thermophilus, K. polysporous* and *H. sapiens* (see Figure 2 for details).

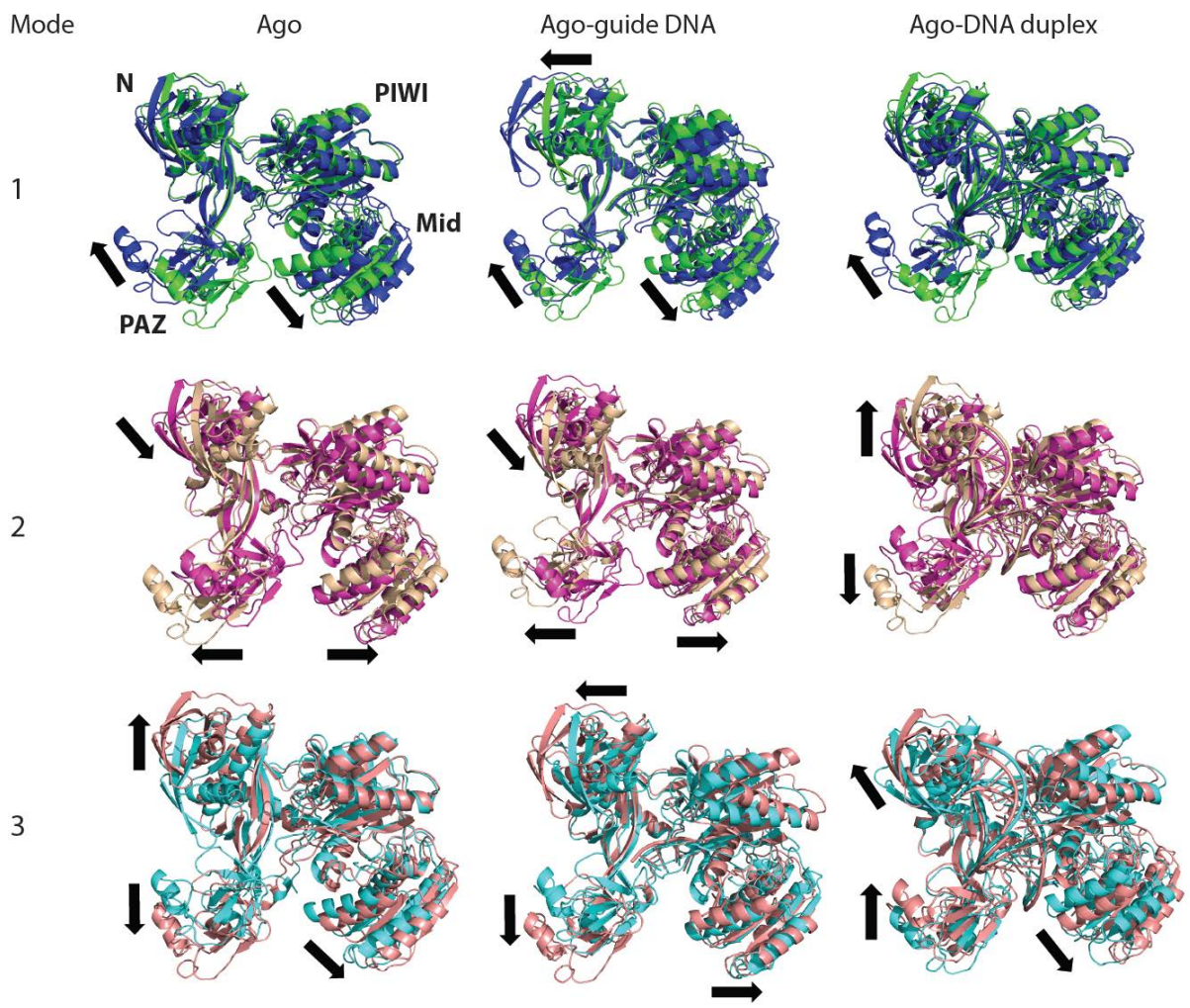

Supplementary Figure S4. Low-frequency conformational dynamics of *T. thermophilus* Ago-RNA complexes. All complexes are derived from the same crystal structure (4NCB). Ago and Ago-guide DNA (8 nt) complexes have similar dynamic modes, but low-frequency Ago-DNA duplex motions (modes 1 and 2) are restricted to the N terminal and PAZ domains, indicating that the complex is stabilized by the duplex.

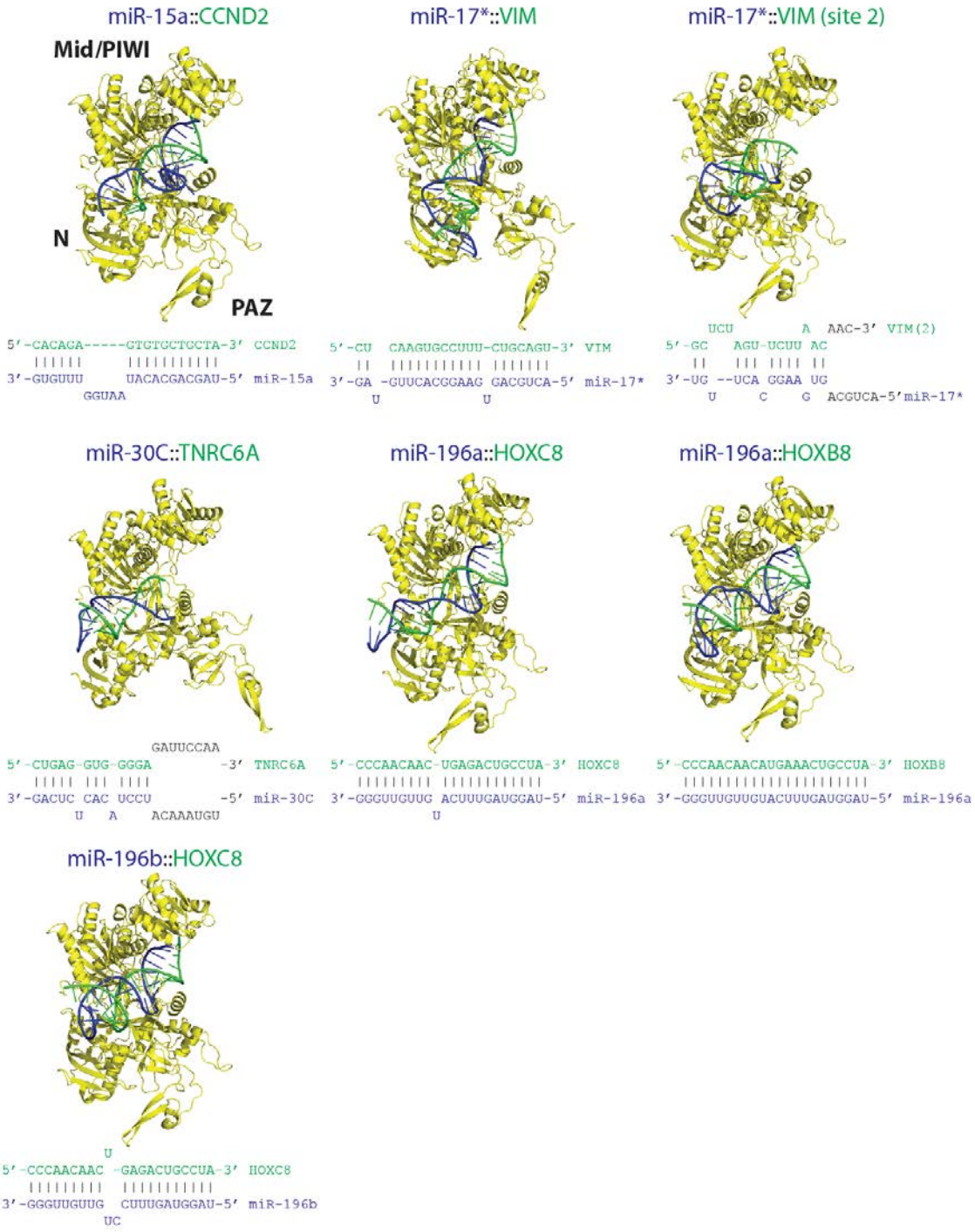

Supplementary Figure S5. Models of human AGO1 miRISC structures. See Figure 4 for details. For seedless targets, as defined by fewer than four base pairs within the first 8 bases of the miRNA, only the structured part of the duplex was modeled. Color scheme: Ago, yellow; guide RNA strand, blue; mRNA strand, green; and unmodeled RNA bases, black.

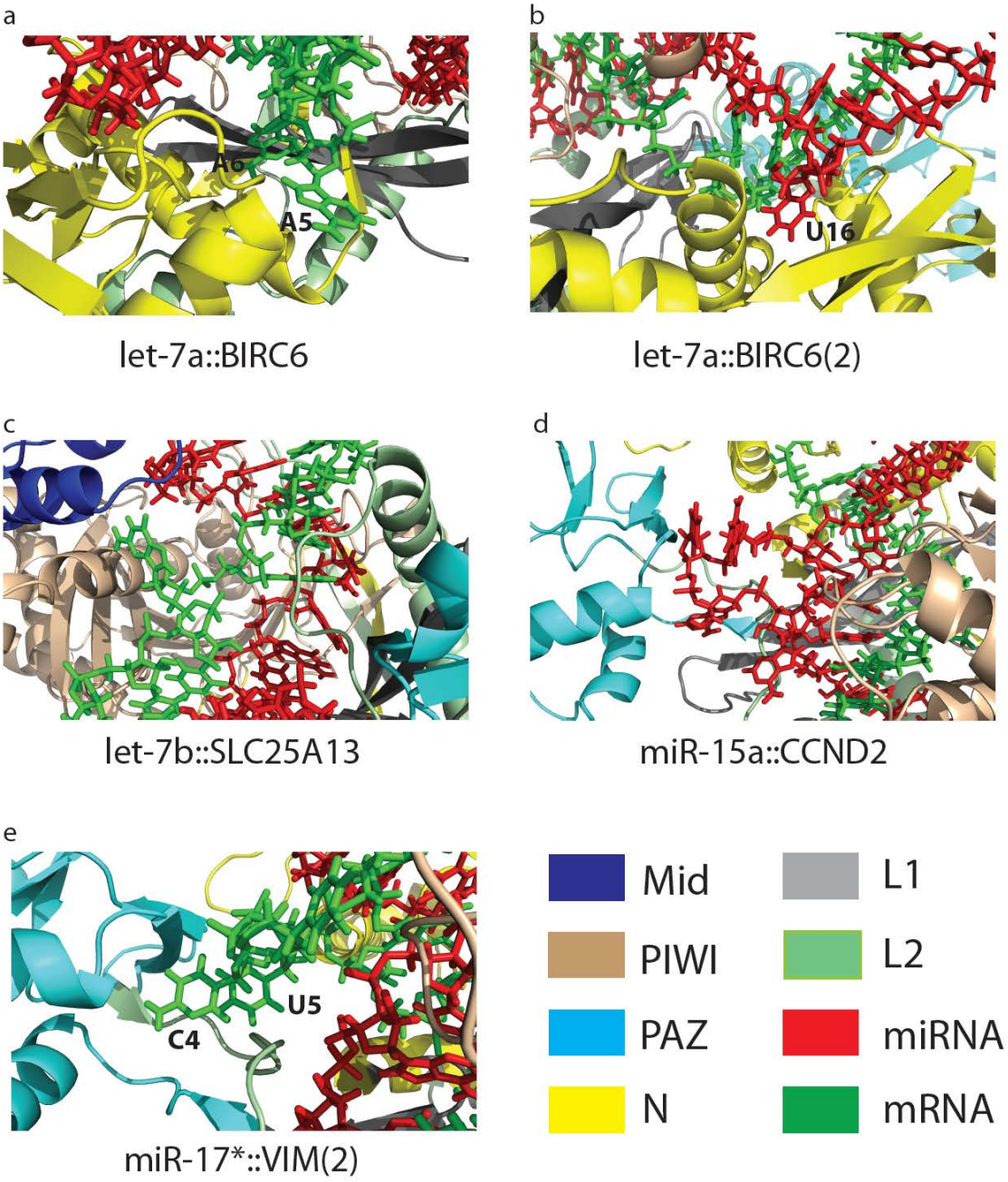

Supplementary Figure S6. Detailed views of the accommodation of duplex imperfections by human AGO1 structures. (a) Insertion of two flipped out A5 and A6 bases of mRNA into a pocket formed by the N terminal group and linker L1. (b) Insertion of the flipped out U16 base of miRNA into a pocket of the N terminal group. (c) Interactions of multiple unpaired bases in the internal loop formed by miRNA and mRNA strands with AGO1's linker L2 and PIWI and PAZ domains. (d) Interactions of multiple unpaired miRNA bases in the internal loop with the PAZ domain of AGO1. (e) Insertion of two flipped out mRNA bases C4 and U5 into a pocket formed by the PAZ domain and linker L2.

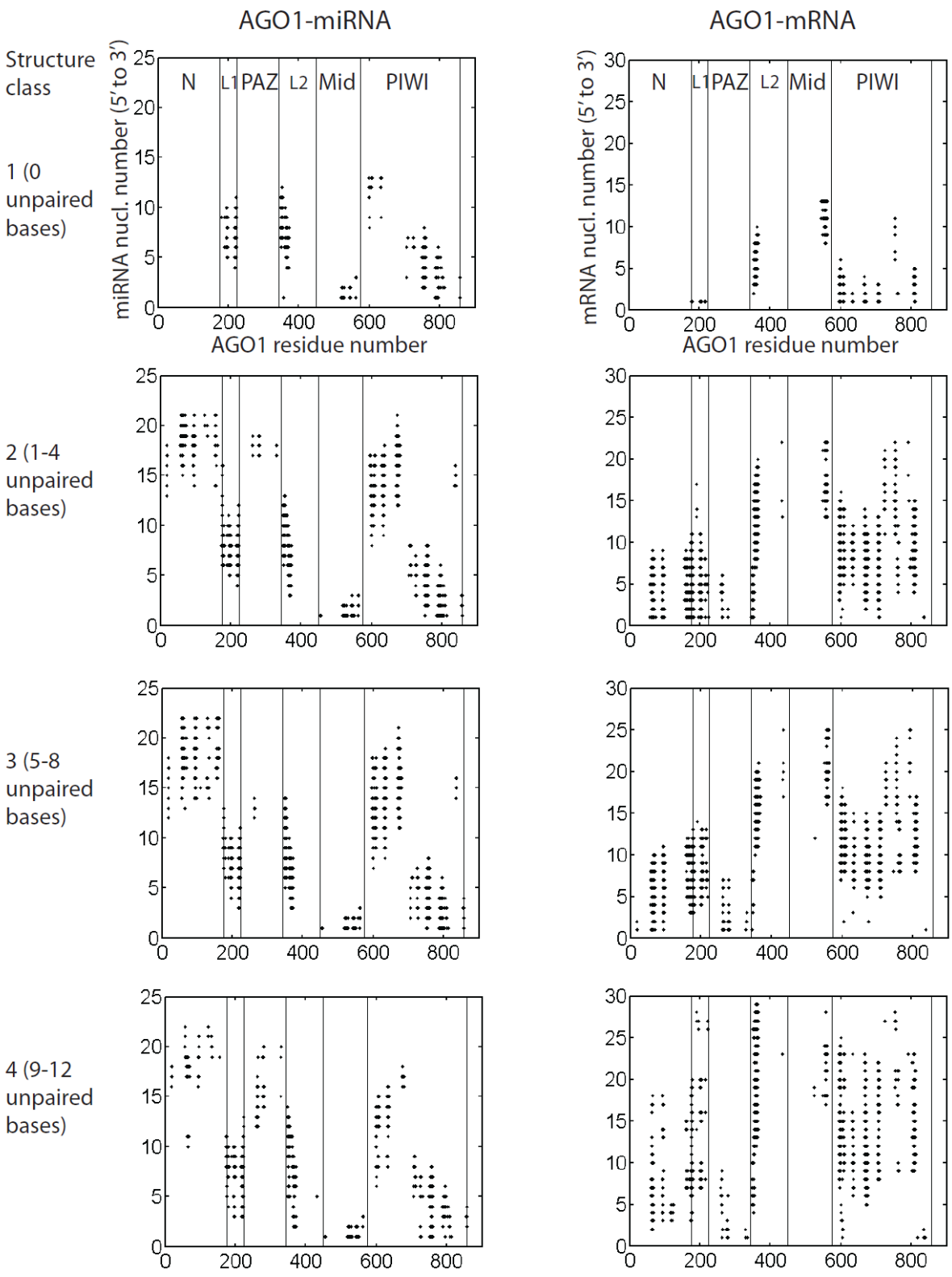
AGO1-miRNA
AGO1-mRNA
Structure class
1 (0 unpaired bases)
2 (1-4 unpaired bases)
3 (5-8 unpaired bases)
4 (9-12 unpaired bases)
miRNA nucl. number (5′ to 3′)
mRNA nucl. number (5′ to 3′)
AGO1 residue number
N
L1
PAZ
L2
Mid
PIWI

Supplementary Figure S7. Residue-level contact maps of human AGO1-miRNA and AGO1-mRNA interactions for four miRNA-mRNA duplex classes differing by the number of unpaired bases (0, 1-4, 5-8, 9-12). 78 duplexes from chimeric miRNA-mRNA reads (targets in Table S3 of Helwak et al. (2013) Cell, 153, 654-665) were used as a basis for constructing AGO1-duplex complexes; we considered only the best fitting complexes (i.e., with the lowest number of atomic overlaps). A pair of protein-RNA residues is considered to be in contact when their C_α-O5' distance is less than 10 Å; protein-protein and RNA-RNA residue contacts are not displayed. The contact maps for duplex structure classes 1-4 are represented by 8, 28, 26 and 15 AGO1-duplex complexes respectively. These maps show that class 1 structures or perfect duplexes (row 1) exhibit localized interactions between their miRNA strands and AGO1's L1, L2, Mid, PIWI domains, whereas imperfect duplexes (classes 2-4) display broad distributions in their interactions with the N terminal and other domains, thus indicating that duplex structure distortions generated many alternative Ago-RNA interactions.

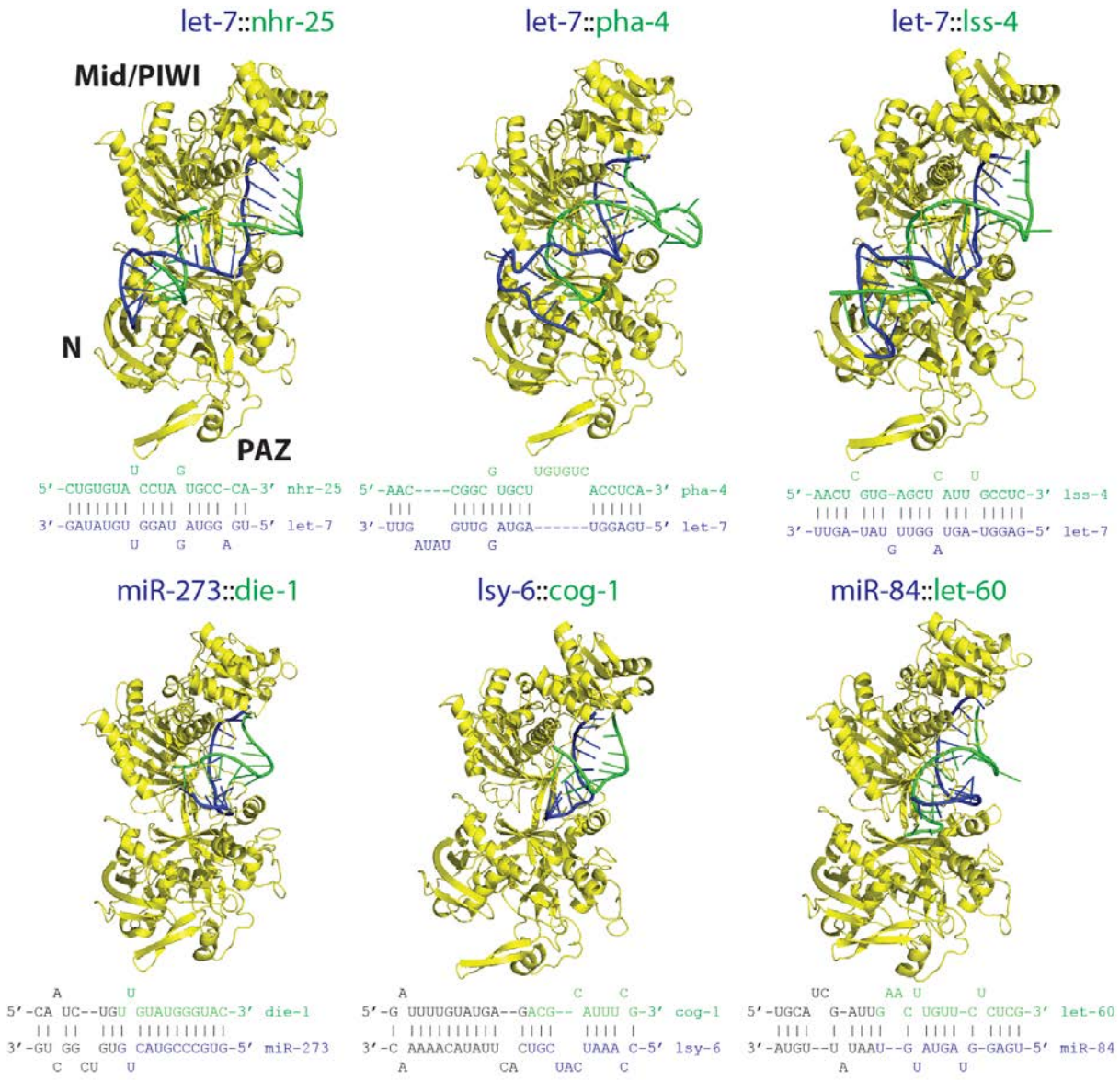

Supplementary Figure S8. Models of *C. elegans* miRISC structures. See Figure 6 for details, except that these duplexes are only partially accommodated in the complexes. Color scheme: Ago, yellow; guide RNA strand, blue; mRNA strand, green; and unmodeled RNA bases, black.